Available online at www.sciencedirect.com

ScienceDirect

Procedia Structural Integrity 2 (2016) 1367–1374

Structural Integrity Procedia

www.elsevier.com/locate/procedia

21st European Conference on Fracture, ECF21, 20-24 June 2016, Catania, Italy

Interfacial fracture strength property of micro-scale SiN/Cu components

Yoshimasa Takahashi[a,*], Kazuya Aihara[a], Itaru Ashida[a], Masanori Takuma[a], Kenichi Saitoh[a], Tomohiro Sato[a], Kimitaka Higuchi[b], Yuta Yamamoto[b], Shigeo Arai[b], Shunsuke Muto[b]

[a]*Department of Mechanical Engineering, Kansai University, 3-3-35 Yamate-cho, Suita-shi, Osaka 564-8680, Japan*
[b]*Institute of Materials and Systems for sustainability (IMaSS), Nagoya University, Furo-cho, Chikusa-ku, Nagoya 464-8603, Japan*

Abstract

The strength against fracture nucleation from an interface free-edge of silicon-nitride (SiN)/copper (Cu) micro-components is evaluated. A special technique that combines a nano-indenter specimen holder and an environmental transmission electron microscope (E-TEM) is employed. The critical load at the onset of fracture nucleation from a wedge-shaped free-edge (opening angle: 90°) is measured both in a vacuum and in a hydrogen (H_2) environment, and the critical stress distribution is evaluated by the finite element method (FEM). It is found that the fracture nucleation is dominated by the near-edge elastic singular stress field that extends about a few tens of nanometers from the edge. The fracture nucleation strength expressed in terms of the stress intensity factor (K) is found to be eminently reduced in a H_2 environment.

Keywords: Micro-components; Silicon-nitride; Copper; Interface free-edge; Fracture nucleation; Hydrogen; Transmission electron microscope

1. Introduction

Advanced micro-devices such as large-scale integration (LSI) or micro-electromechanical systems (MEMS), as they are fabricated via multi-step mask-etching/deposition processes, contain many micron/ submicron-scale structural components and their interfaces. The structural integrity of these devices then depends strongly on the

* Corresponding author. Tel.: +81-6-6368-0748; fax: +81-6-6368-0748.
E-mail address: yoshim-t@kansai-u.ac.jp

10.1016/j.prostr.2016.06.174

Nomenclature

p_{H2}	partial pressure of hydrogen gas (kPa)
F	applied load (μN)
F_c	critical load at fracture nucleation (μN)
E	Young's modulus (GPa)
ν	Poisson's ratio
C_{11}, C_{12}, C_{44}	anisotropic constants (GPa)
t	time (s)
σ_x	normal stress along SiN/Cu interface (MPa)
τ_{xy}	shear stress along SiN/Cu interface (MPa)
r	distance from SiN/Cu interface free-edge (nm)
θ	angle measured from SiN/Cu interface (rad.)
λ	stress singularity index
K	stress intensity factor (MPa m^{λ})
K_c	critical stress intensity factor at fracture nucleation (MPa m^{λ})
σ_{ij}	stress tensor
f_{ij}	non-dimensional function of θ

strength of interfaces that abound with various kinds of defects (e.g. misfit dislocations, voids, alloyed layers).

The mechanical strength of an interface is generally discussed either in terms of the crack growth resistance (toughness) or in terms of the resistance against fracture nucleation from, e.g., a "free-edge" where the interface meets a free-surface. From an engineering viewpoint, both events (nucleation and growth) are important as they often occur on the same interface in sequence. The interfacial toughness of low-dimensional micro-components is mostly evaluated by simulated tests using relatively large specimens (e.g. four-point bending test of a film-deposited substrate with a pre-crack introduced along the target interface, see e.g. Maidenberg et al. (2004) or Hirakata et al. (2010)). On the other hand, the interfacial fracture nucleation strength of micro-components needs to be directly evaluated by using micro-scale specimens because it is essentially difficult to fabricate large specimens simulating the target interface edges.

Several methods have been developed to evaluate the interfacial fracture nucleation strength of micro-components: a laterally scanned nano-indenter tip attached to an atomic force microscope (AFM) was utilized to delaminate micro-dots on a substrate by Hirakata et al. (2006), multi-layered micro-columns were laterally loaded and delaminated under scanning electron microscopy (SEM) by Kamiya et al. (2013), multi-layered micro-cantilevers were bended and delaminated under transmission electron microscopy (TEM) by, e.g., Sumigawa et al. (2010), Kawai et al. (2014). These experiments, however, were conducted either in vacuum or in ambient air. The authors have then proposed a novel experimental technique that combines an environmental TEM (E-TEM) and a nano-indenter apparatus (Takahashi et al. (2015a)): it allows fracture behavior observation and load measurement simultaneously in various types of gaseous environments.

In this study, the strength against fracture nucleation from the free-edge of silicon nitride (SiN)/copper (Cu) micro-components is focused. This material combination typically finds its application in LSI devices (e.g. interconnect/barrier layer). The effect of environment, particularly hydrogen (H_2), on the fracture strength is also investigated.

2. Materials and methods

The micro-scale specimens containing interfaces of different materials were fabricated from multilayered thin films deposited on a single-crystalline silicon (Si) substrate. The native oxide on a (001) Si wafer was firstly removed by argon (Ar) sputtering. Then a Cu film and a SiN film were sequentially deposited by magnetron sputtering under Ar gas pressure of 0.67 Pa. Cu and SiN were polycrystalline and amorphous respectively, and the nominal thicknesses were 200 nm and 500 nm, respectively.

Figure 1 schematically shows the fabrication procedure of a specimen. An amorphous carbon (C) layer, whose size was ca. 10 μm × 10 μm × 1 μm, was deposited with focused ion beam (FIB) on the SiN film. A trench surrounding the C layer was milled. The sample stage was then tilted and a bottom trench was milled. The block was lifted out from the substrate by a solid probe and then transported to the flattened end of a metal wire. A thin membrane, whose thickness was ca. 400–500 nm, was milled from the block. A lever-shaped specimen having interfaces was formed. Finally, a wedge-shaped notch (opening angle: 90°) was introduced at the target interface. All these processes were carefully monitored with secondary electron images of a dual-channel FIB system (SMI-3050SE, SII Ltd.). The beam acceleration for gallium (Ga) ion and electron was 30 kV and 5 kV, respectively. An example of the SEM image of a specimen is shown in Fig. 2.

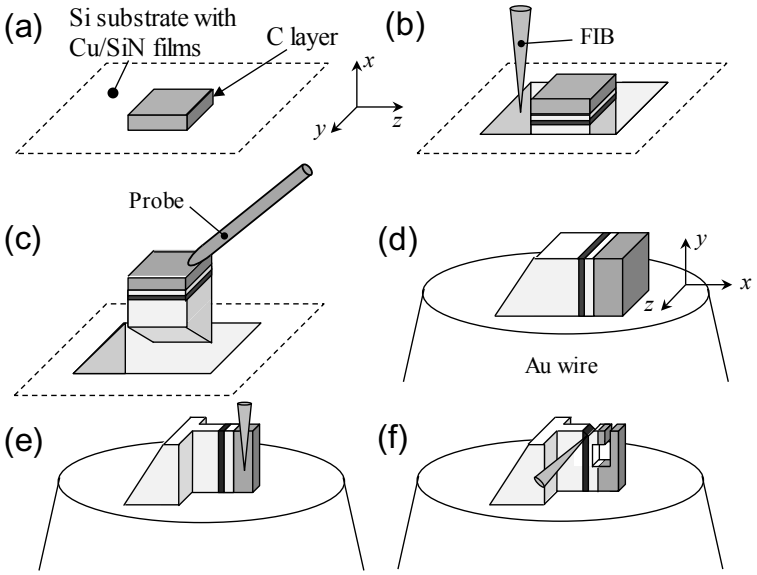

Fig. 1. Fabrication procedure of a micro-specimen containing interfaces: (a) carbon layer deposition; (b) trenching; (c) pick up; (d) stage mounting; (e) thinning; (f) lever shaping and notch introduction.

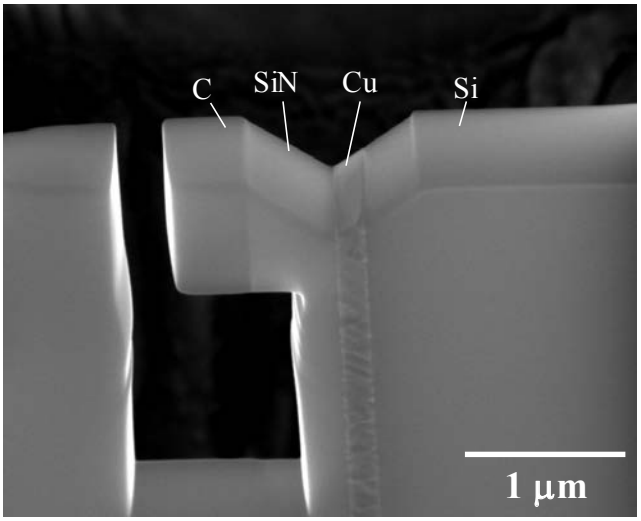

Fig. 2 SEM photograph of a micro-specimen with a wedge-shaped free-edge.

The fracture tests were conducted by using a nano-indenter specimen holder (HN200E, Nanofactory Instruments AB). The metal wire with specimens was attached to the piezo-driven sample stage of the holder. In the TEM column, the micro-cantilever specimen was moved toward a diamond indenter with pyramidal head shape. After the preliminary positioning, the C layer of the cantilever was pressed by the indenter. The piezo displacement was manually increased in a stepwise manner (minimum step: 1 nm) at a constant speed (1 nm s^{-1}). The diamond indenter is attached on a micro-load sensor whose load range and precision (floor noise) are 3 mN and 0.74 μN (rms), respectively. The sampling period of the load value was 0.125 s. TEM image was recorded at a frame rate of 30 s^{-1}.

The tests were conducted in a special E-TEM facility (Reaction-Science High-Voltage Electron Microscope; RSHVEM) at Nagoya University, Japan (JEM-1000K RS, JEOL Ltd.). In the case of tests in a gaseous environment, an environmental cell (EC) was inserted to the objective pole piece gap, and a local gas environment was formed at the holder head. For more detailed specification of this facility, see Tanaka et al. (2013) and Takahashi et al. (2015). In this study, H_2 gas diluted with nitrogen (N_2) gas was admitted to the EC, and the partial pressure of H_2 (p_{H2}) was controlled at 1 kPa. In the case of tests in a vacuum environment, the EC was retracted from the column. Note that the effective pressure (fugacity) of ionized gas is known to be significantly higher than the actual gas pressure; dry H_2 gas in an EC, whose pressure is kept between 10-16 kPa, is estimated by Bond et al. (1986) to have fugacity that exceeds 40 MPa when an acceleration voltage of 200 kV is employed.

After the tests, the critical stress distribution in the specimens at fracture nucleation was calculated by the finite element method (FEM). Figure 3 shows an example of the FEM model. Only the thinned part of the specimen (see Fig. 1(f)) was modeled, and a symmetry condition with respect to the *xy*-plane was employed. The boundary between the thinned part and the thick block part was fixed. The bottom of the thinned part was also fixed. Specimen dimension in the *xy*-plane was measured by TEM, and the thickness in *z*-direction was measured by SEM. The element size around the interface free-edge was reduced to about 0.02 nm. The load value at fracture nucleation, F_c, was applied to the model ($F_c/2$ due to *xy*-plane symmetry). The material constants are listed in Table 1. Cu, SiN and C were considered to be isotropic elastic body. Si was considered to be orthotropic elastic body. The analyses, including pre/post processes, were conducted by using ABAQUS™ ver. 6.11 (Dassault Systems Ltd.).

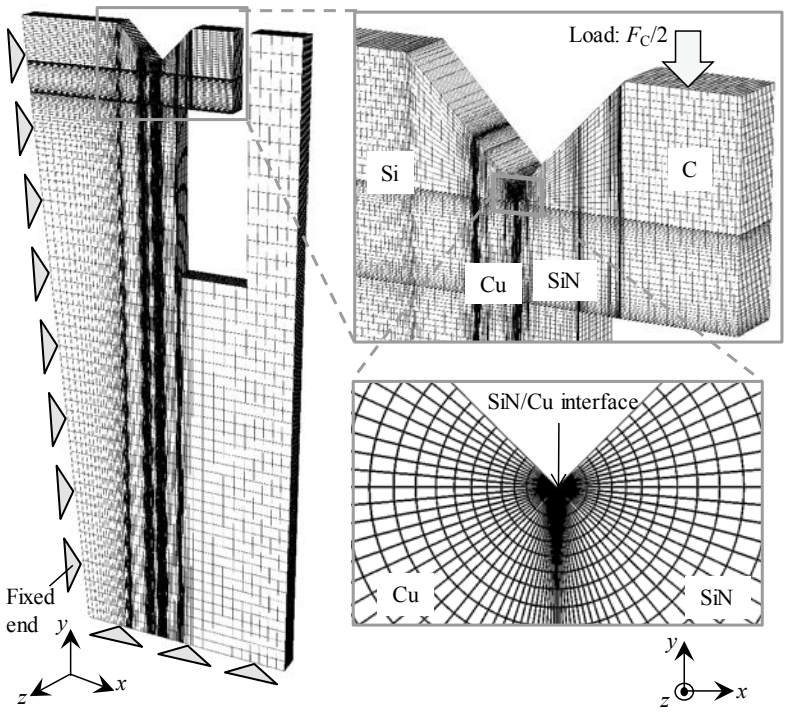

Fig. 3. 3D FEM model for stress analysis.

Table 1. Material constants used in FEM.

Material	Young's modulus E (GPa)	Poisson's ratio ν	Anisotropic constants (GPa)
Silicon nitride (SiN)	304	0.27	–
Copper (Cu)	129	0.34	–
Carbon (C)	400	0.3	–
Silicon (Si)	–	–	C_{11}: 165.8, C_{12}: 63.9, C_{44}: 79.6

3. Results and discussion

3.1. Fracture test

Figure 4 shows an example of load application curve (F - t relation) and the corresponding TEM images at the specified points A, B and C. Since the piezo movement was controlled at a constant rate, the load increased almost linearly with stage displacement. No eminent change was observed in the specimen between points A and B. At point B, the load suddenly dropped and fracture along the SiN/Cu interface was initiated, and the crack was arrested at point C. These events occurred in a single video frame (i.e. within 0.033 s). Then the specimen was unloaded. The F - t relation of all the specimens (in vacuum and H_2 gas) generally showed the same behavior. The peak load at point B (F_c) is then considered as the critical load for fracture nucleation, which is applied to the FEM model in the stress analysis.

3.2. Critical stress distribution

Figure 5 shows examples of the critical stress distribution along SiN/Cu interface. Here, stress normal to the interface and parallel to the interface are denoted as σ_x and τ_{xy}, respectively. Two specimens having relatively large difference of size are compared. The magnitude of near-edge σ_x is much larger than τ_{xy}. In the double logarithmic

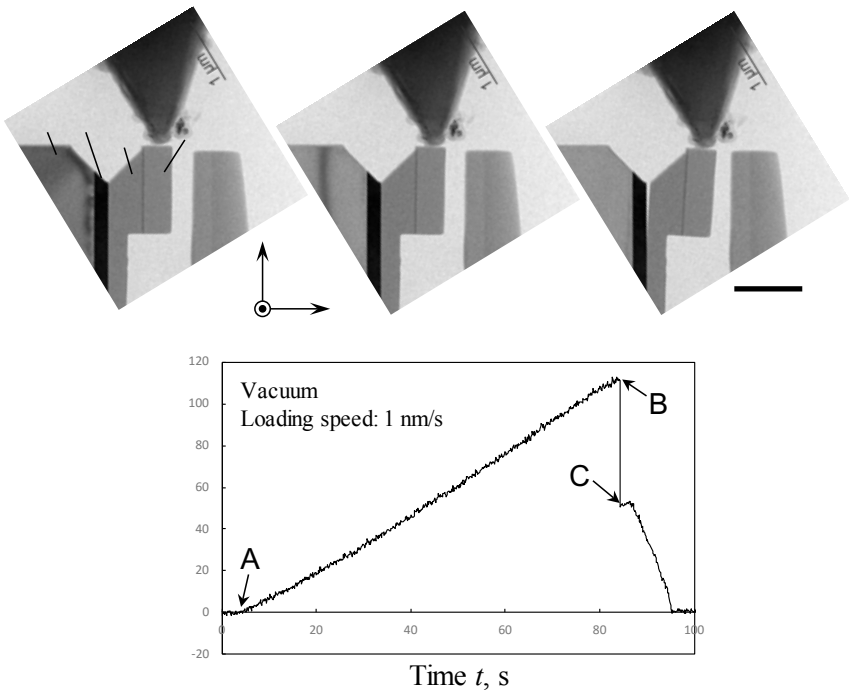

Fig. 4. Example of fracture test: in situ TEM images and the corresponding loading curve (test conducted in vacuum).

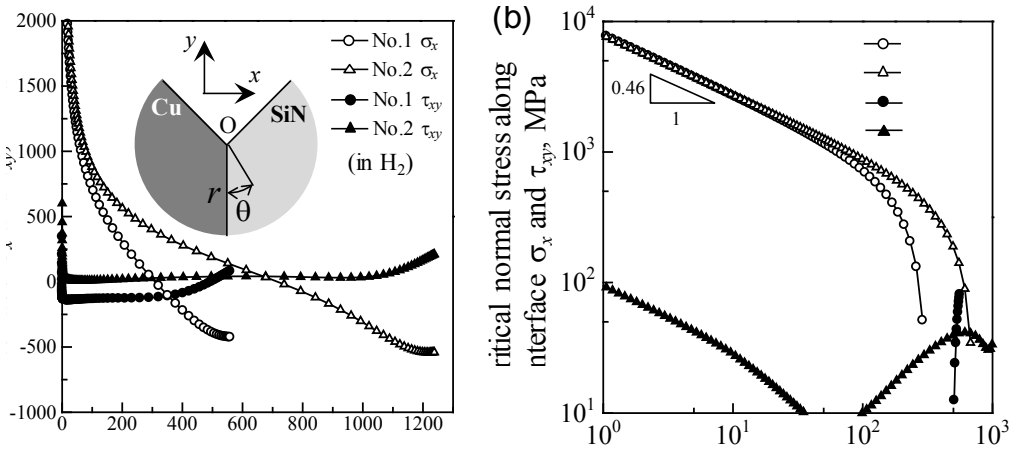

Fig. 5. Critical elastic stress distribution along SiN/Cu interface: (a) linear plot, (b) double logarithmic plot.

plot (Fig. 5(b)), the near-edge σ_x is seen to asymptote approximately to the same linear relation irrespective of the specimen size. Note that τ_{xy} for specimen No.1 (●) in the shown range is mostly negative while it becomes positive when $r < 0.2$ nm. It is therefore postulated that the fracture nucleation from the SiN/Cu free-edge is characterized by the σ_x singular stress field that extends a few tens of nanometers, which is consistent with the results obtained for a different free-edge shape by Kawai et al. (2014).

In terms of the fracture mechanics, the asymptotic elastic stress field near an interfacial free-edge is expressed by Bogy (1968) and Bogy (1971) as follows.

$$\sigma_{ij} = \frac{K}{r^{\lambda}} f_{ij}(\theta) \tag{1}$$

Here, stress tensor, σ_{ij}, is expressed in terms of the polar coordinate (r, θ) originating from the free-edge (see the inset in Fig. 5(a)). K is the stress intensity factor, λ the stress singularity index and f_{ij} the non-dimensional function of θ. Theoretically, there are two λ values for the present material combination and edge shape: $\lambda_1 = 0.46$ and $\lambda_2 = 0.09$. It can be seen that the near-edge stress field in Fig. 5(b) is primarily dominated by the former singularity.

3.3. Fracture nucleation strength (influence of hydrogen)

The strength against fracture nucleation is expressed in terms of the K value here. By fitting the near-edge stress distribution to Eq. (1) with a singularity index of 0.46, K values for all the specimens are evaluated. Figure 6 compares the fracture nucleation strength of specimens tested in vacuum and H_2-containing environment. The strength in the H_2-containing environment is much lower than in vacuum: the reduction of the average strength value is ca. 30%. Birringer et al. (2012) has shown that the existence of H_2 gas enhances the crack growth rate along SiN/Cu interface by conducting single cantilever beam tests of film-deposited substrates. The present results quantitatively confirm that the H_2 gas has eminent influence on the fracture nucleation strength from the SiN/Cu free-edge. These results together imply that the SiN/Cu interface is essentially susceptible to hydrogen embrittlement (HE), which is in marked contrast to other HE-resistant systems (e.g. Si/Cu free-edge investigated by Takahashi et al. (2015b)).

The methodology employed in this study can be applied, e.g., to investigate the effect of free-edge shape (i.e. stress singularity) on HE susceptibility or to compare the HE susceptibility of various material combination. It should be pointed out again, however, that the gaseous environment in the EC, as a high-energy beam (1000 kV) is

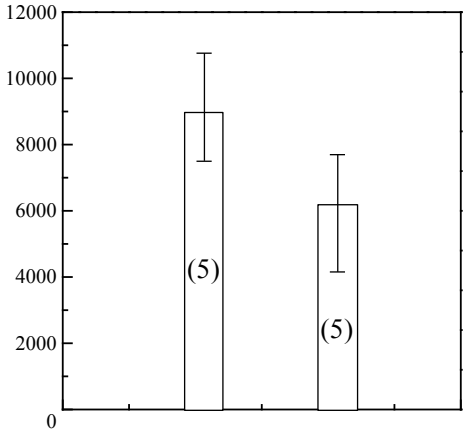

Fig. 6. Comparison of fracture nucleation strength represented by the critical stress intensity factor, K_c. The number in the parenthesis indicates the total number of specimens.

illuminated, is far more active than an ordinary environment. The calibration of the effective pressure in EC would then be required if the present data were to be compared to that obtained under a normal molecular gas.

4. Summary

In this study, the strength against fracture nucleation from the silicon-nitride (SiN)/copper (Cu) interface free-edge contained in micro-components was evaluated. An experimental technique that combines a nano-indenter specimen holder for a transmission electron microscope (TEM) and a special high-voltage TEM equipped with an environmental cell (EC) was employed. The critical load at the onset of fracture nucleation from a wedge-shaped free-edge (opening angle: 90°) was measured both in a vacuum environment and in a hydrogen (H_2) environment. The critical stress distribution was then evaluated by the finite element method (FEM). It was found that the fracture nucleation was dominated by the near-edge elastic singular stress field that extends about a few nanometers from the edge. The fracture nucleation strength expressed in terms of the stress intensity factor (K) was found to be eminently reduced in a H_2 environment.

Acknowledgements

The present study was performed under the auspices of Reaction science/Nanomaterials science Research support base of Microstructure Analysis Platform in ‘Nanotechnology Platform Project’ by the Ministry of Education, Culture, Sports, Science and Technology (MEXT), Japan. Y. T. of the authors is also grateful to financial support by the Japan Society for the Promotion of Science (JSPS) KAKENHI Nos. 25709003 (Grant-in-Aid for Young Scientists A), 25000012 (Specially Promoted Research).

References

Birringer, R.P., Shaviv, R., Besser, P.R., Dauskardt, R.H., 2012. Environmentally Assisted Debonding of Cu/Barrier Interfaces. Acta Materialia 60, 2219–2228.

Bogy, D.B., 1968. Edge-Bonded Dissimilar Orthogonal Elastic Wedges under Normal and Shear Loading. Journal of Applied Mechanics 35, 460–466.

Bogy, D.B., 1971. Two Edge-Bonded Elastic Wedges of Different Materials and Wedge Angles under Surface Tractions. Journal of Applied Mechanics 38, 377–386.

Bond, G.M., Robertson, I.M., Birnbaum, H.K., 1986. On the Determination of the Hydrogen Fugacity in an Environmental Cell TEM Facility. Scripta Metallurgica 20, 653–658.

Hirakata, H., Takahashi, Y., Matsumoto, S., Kitamura, T., 2006. Dominant Stress Region for Crack Initiation at Interface Edge of Microdot on a Substrate. Engineering Fracture Mechanics 73, 2698–2709.

Hirakata, H., Yamada, T., Nobuhara, Y., Yonezu, A., Minoshima, K., 2010. Hydrogen Effect on Fracture Toughness of Thin Film/Substrate Interfaces. Engineering Fracture Mechanics 77, 803–818.

Kamiya, S., Shishido, N., Watanabe, S., Sato, H., Koiwa, K., Omiya, M., Nishida, M., Suzuki, T., Nakamura, T., Nokuo, T., Nagasawa, T., 2013. Grain-scale Adhesion Strength Mapping of Copper Wiring Structures in Integrated Circuits. Surface and Coatings Technology 215, 280–284.

Kawai, E., Sanada. K., Sumigawa, T., Kitamura, T., 2014. Delamination Crack Initiation from Copper/Silicon Nitride Interface Edge with Nanoscale Singular Stress Field. Engineering Fracture Mechanics 120, 60–66.

Maidenberg, D.A., Volksen, W., Miller, R.D., Dauskardt, R.H., 2004. Toughning of Nanoporous Glasses using Porogen Residuals. Nature Materials 3, 464–469.

Sumigawa, T., Shishido, T., Murakami, T., Kitamura, T., 2010. Interface Crack Initiation due to Nano-Scale Stress Concentration. Materials Science and Engineering A 527, 4796–4803.

Takahashi, Y., Arai, S., Yamamoto, Y., Higuchi, K., Kondo, H., Kitagawa, Y., Muto, S., Tanaka, N., 2015a. Evaluation of Interfacial Fracture Strength in Micro-Scale Components Combined with High-voltage Environmental Electron Microscopy, Experimental Mechanics 55, 1047–1056.

Takahashi, Y., Aihara, K., Ashida, I., Higuchi, K., Yamamoto, Y., Arai, S., Muto, S., Tanaka, N., 2015b. Evaluation of interfacial fracture strength in micro-components with different free-edge shape, International Conference on Advanced Technology in Experimental Mechanics (ATEM). Toyohashi, Japan, p. 192.

Tanaka, N., Usukura, J., Kusunoki, M., Saito, Y., Sasaki, K., Tanji, T., Muto, S., Arai, S., 2013. Development of an Environmental High-voltage Electron Microscope for Reaction Science. Microscopy 62, 205–215.